Supporting Information

Ultra-high-density 3D DNA arrays within nanoporous biocompatible membranes for single-molecule-level detection and purification of circulating nucleic acids

M. Aramesh,*[a,d] O. Shimoni,[a,b] K. Fox,[a,c] T.J. Karle,[a] A. Lohrmann,[a] K. Ostrikov,[d,e] S. Prawer*[a] and J. Cervenka[a,f]

[a] School of Physics, The University of Melbourne, Melbourne, Victoria 3010, Australia.
[b] School of Physics and Advanced Materials, University of Technology, Sydney, New South Wales 2007, Australia.
[c] School of Aerospace, Mechanical and Manufacturing Engineering, RMIT University, Carlton, VIC 3053, Australia.
[d] Plasma Nanoscience Laboratories, Commonwealth Scientific and Industrial Research Organisation (CSIRO), PO Box 218, Lindfield, NSW 2070, Australia.
[e] School of Chemistry, Physics, and Mechanical Engineering, Queensland University of Technology, Brisbane QLD 4000, Australia.
[f] Institute of Physics ASCR, v. v. i., Cukrovarnicka 10, Prague 6, Czech Republic.

* Corresponding authors:
mrtz.aramesh@gmail.com, s.prawer@unimelb.edu.au

Method	Material	Detection limit/concentration	Reference*
Electrical	Flat Graphene	100 fM	1
Electrical	Nanoporous AAO	10 μM	2
PL	Flat silicon/silica	0.1–1 pmol cm^{-2}	3
PL	Nanoporous Silica	70–90 pmol cm^{-2}	4
PL	Nanoporous AAO	100 mM	5
PL	Nanoporous DLC-AAO	Single molecule	This work
SPR	Nanoporous AAO	10 pM	6
RIfS	Nanoporous AAO	2 nmol cm^{-2}	7

Table S1. A comparison between the sensor detection limits of the nanoporous DLC-AAO and some other DNA sensors.

References:

1 G. Xu, J. Abbott, L. Qin, K. Y. M. Yeung, Y. Song, H. Yoon, J. Kong and D. Ham, *Nature communications*, 2014, **5**.

2 X. Wang and S. Smirnov, *ACS Nano*, 2009, **3**, 1004-1010.

3 M. Glazer, J. A. Fidanza, G. H. McGall, M. O. Trulson, J. E. Forman, A. Suseno and C. W. Frank, *Analytical biochemistry*, 2006, **358**, 225-238.

4 M. I. Glazer, J. A. Fidanza, G. H. McGall, M. O. Trulson, J. E. Forman and C. W. Frank, *Biophysical journal*, 2007, **93**, 1661-1676

5 C. L. Feng, X. H. Zhong, M. Steinhart, A. M. Caminade, J. P. Majoral and W. Knoll, *Advanced Materials*, 2007, **19**, 1933-1936.

6 D.-K. Kim, K. Kerman, M. Saito, R. R. Sathuluri, T. Endo, S. Yamamura, Y.-S. Kwon and E. Tamiya, *Analytical chemistry*, 2007, **79**, 1855-1864.

7 S. Pan and L. J. Rothberg, *Nano letters*, 2003, **3**, 811-814

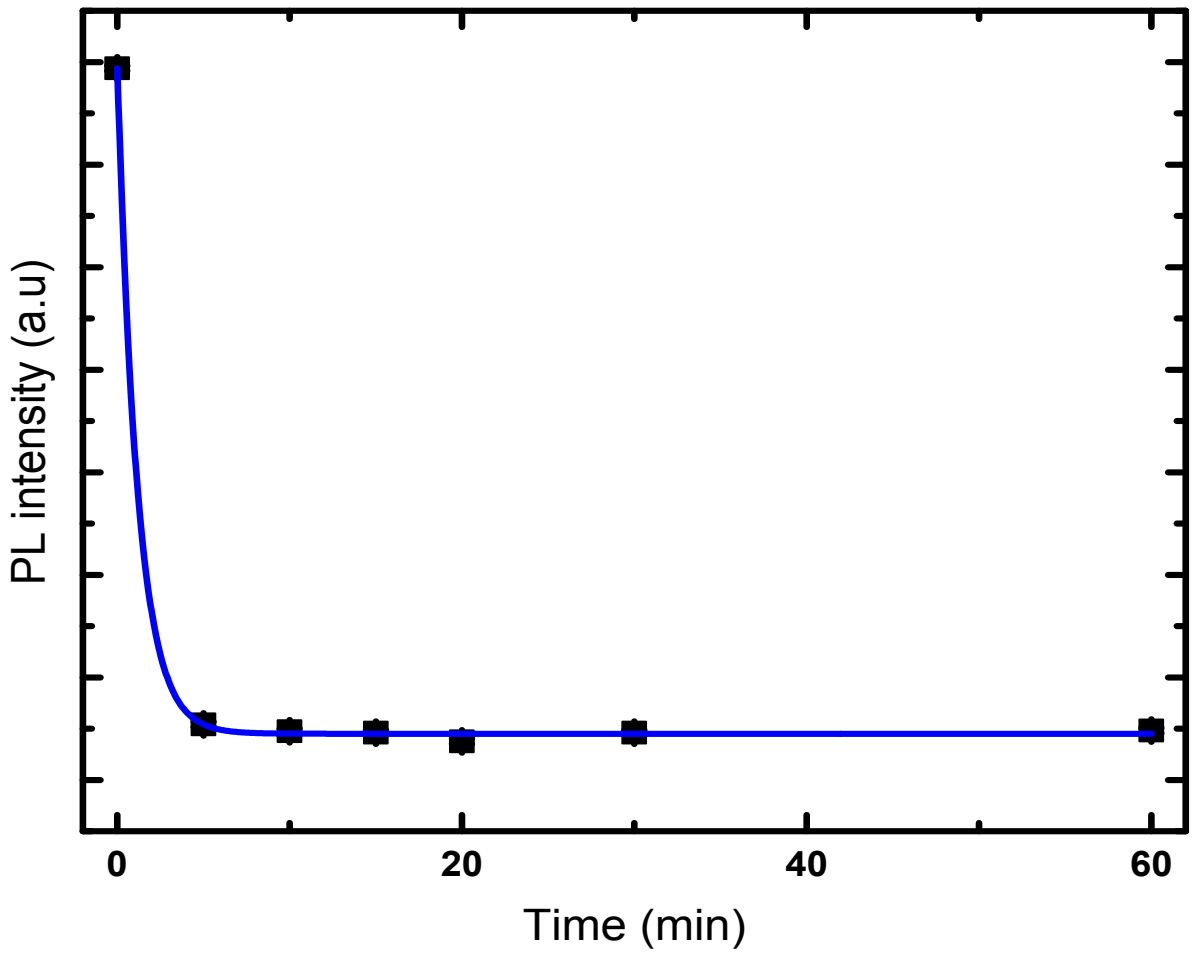

Figure S1. Time dependent fluorescence intensity measurements of the DNA hybridization process in a DLC-AAO membrane. The equilibrium is reached within 10 min.

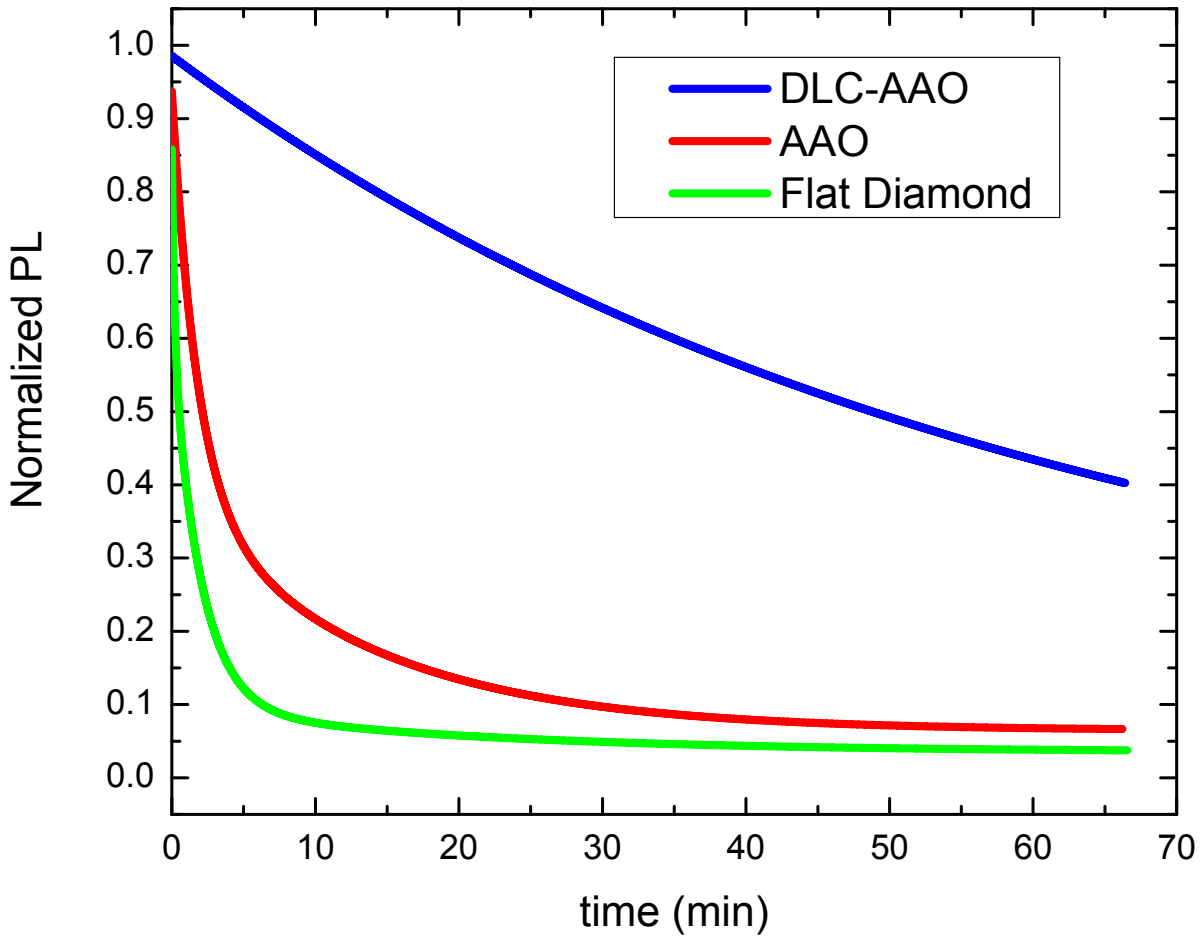

Figure S2. Normalized photoluminescence (photon counts) versus time for different samples at their saturation of target cDNA attached to the surface via hybridization. The photon counts were measured using a confocal microscope connected to an APD. The (double-) exponential decay of the fluorescent emission is obvious from the figures. This decay is attributed to the bleaching of the fluorophores. The signal intensity from the nanoporous DLC-AAO array is dramatically higher than the flat diamond array.

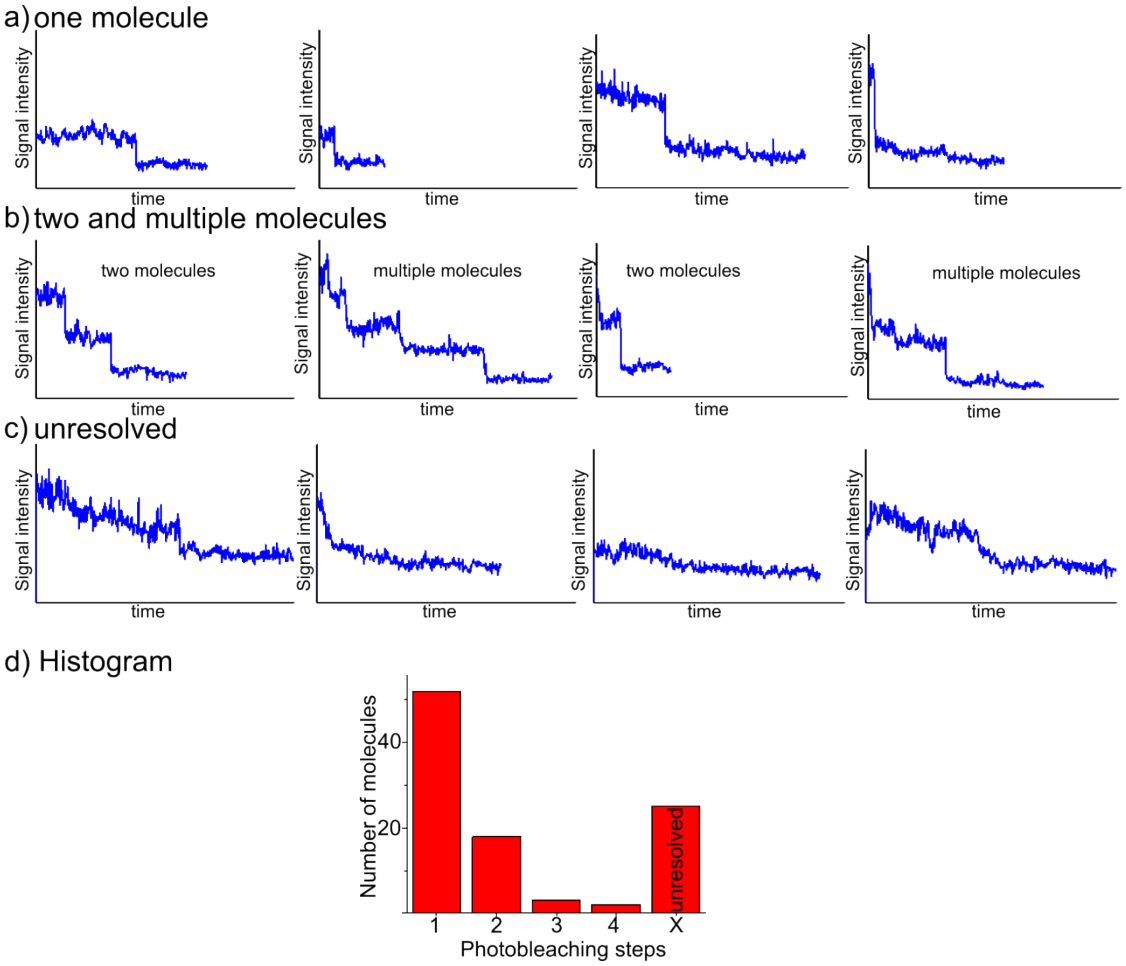

Figure S3. Sample fluorophore time traces depicting (a) one-, (b) two- or multiple-step photobleaching, and (c) unresolved fluorescent intensity levels. Signal intensities and bleaching times are not necessary identical for different fluorophores because of their different (1) depth, (2) background signals, and (3) exposure-history. The unresolved data may arise due to a low signal-to-noise ratio, non-radiative emissions or even chemical variations. (d) Histogram distribution of 100 recorded bleaching observations. Most of the single-spots are single-molecules (>50 %). The rest of the events are identified as two and multiple molecules. Spots with unresolved characteristics (~25%) are marked as X.

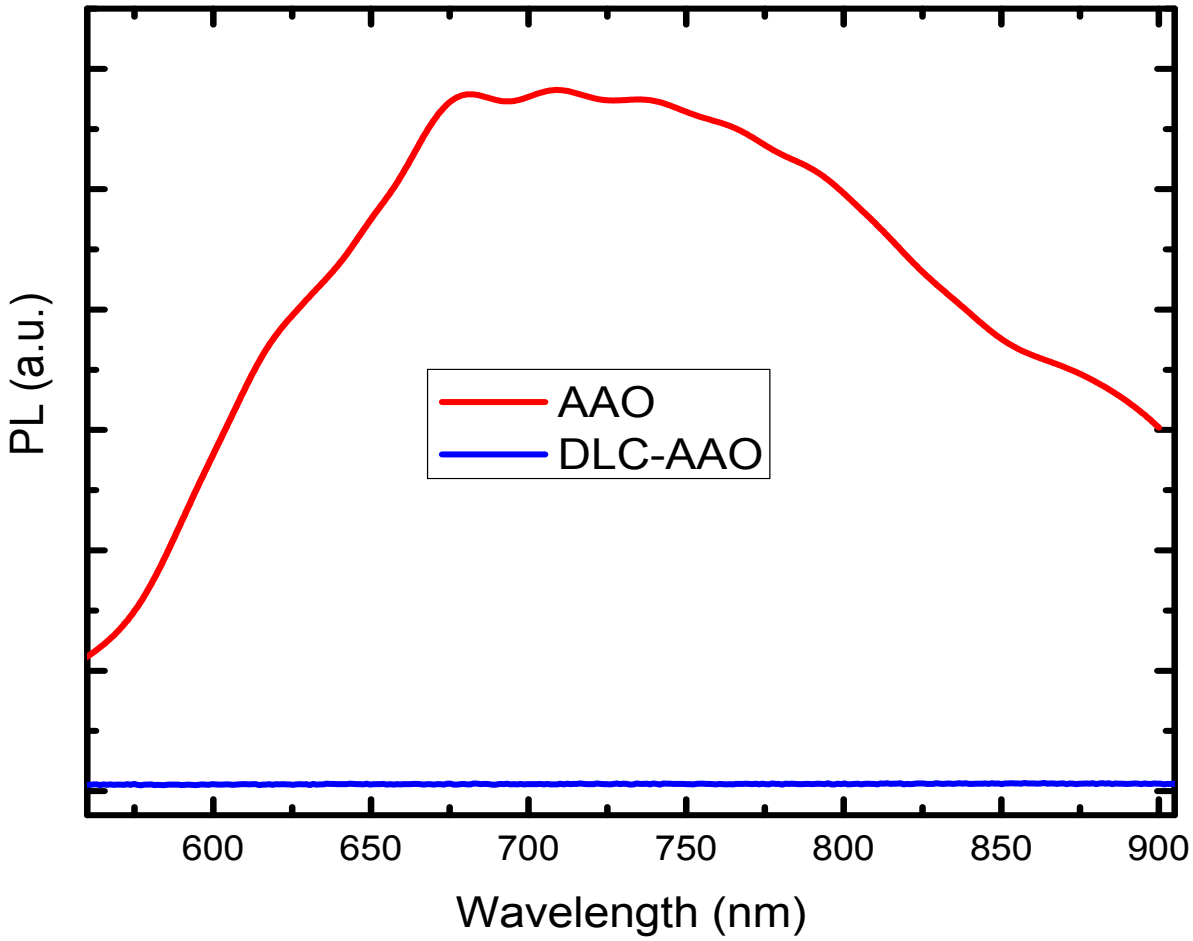

Figure S4. Photoluminescence of AAO and DLC-AAO measured by a 532 nm laser. DLC coating passivates the fluorescent centers on the surface of AAO.

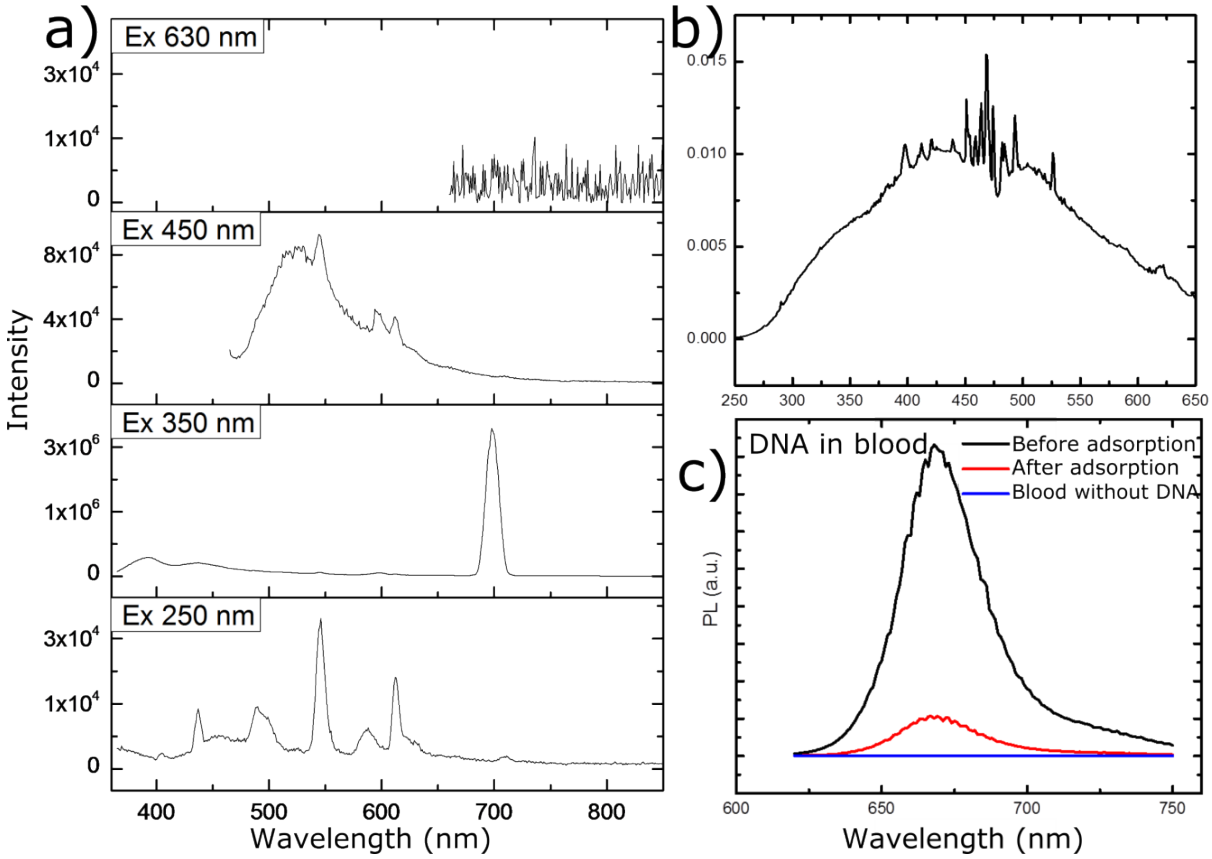

Figure S5. Optical properties of the whole-blood. a) Optical emission from the whole-blood as a function of different excitation wavelengths (250, 350, 450 and 630 nm). It is important to note that there is no significant emission from the blood at the emission of Alexa Fluor 647 when excited with a 630 nm wavelength. b) Optical absorption of the blood when excited with 630 nm light. c) Optical emission of the molecular dye (Alexa Fluor647) when mixed with blood. This result shows that the dye emission does not interfere with the different blood components. Also the reduced emission after DNA adsorption to the sensors, suggests the functionality of the sensor in blood.

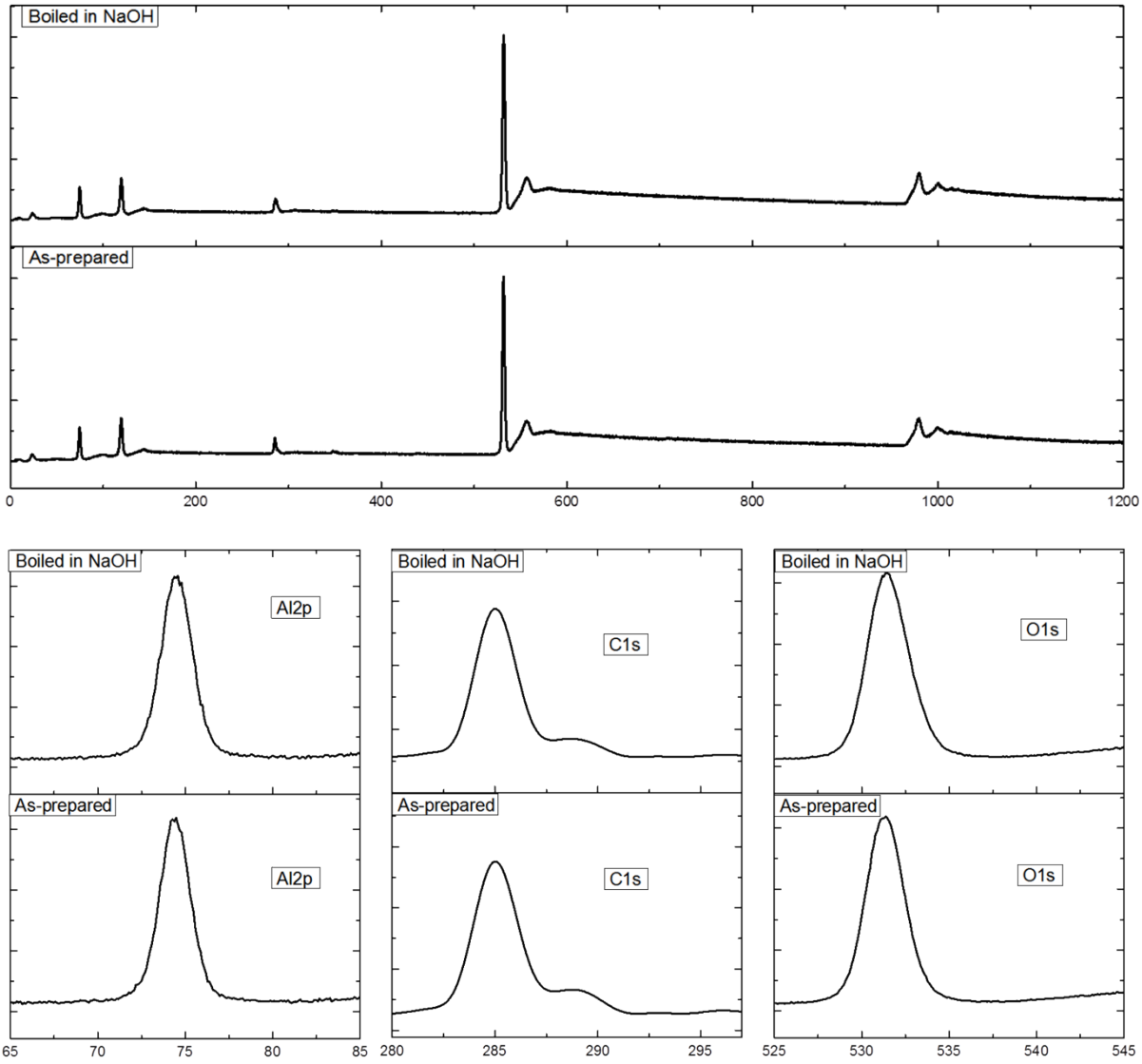

Figure S6. X-ray photoemission spectroscopy (XPS) of the DLC-AAO membranes before and after cleaning with strong alkali (boiling NaOH). It is observed that the surface chemistry of DLC-AAO membrane has not changed by the cleaning step.

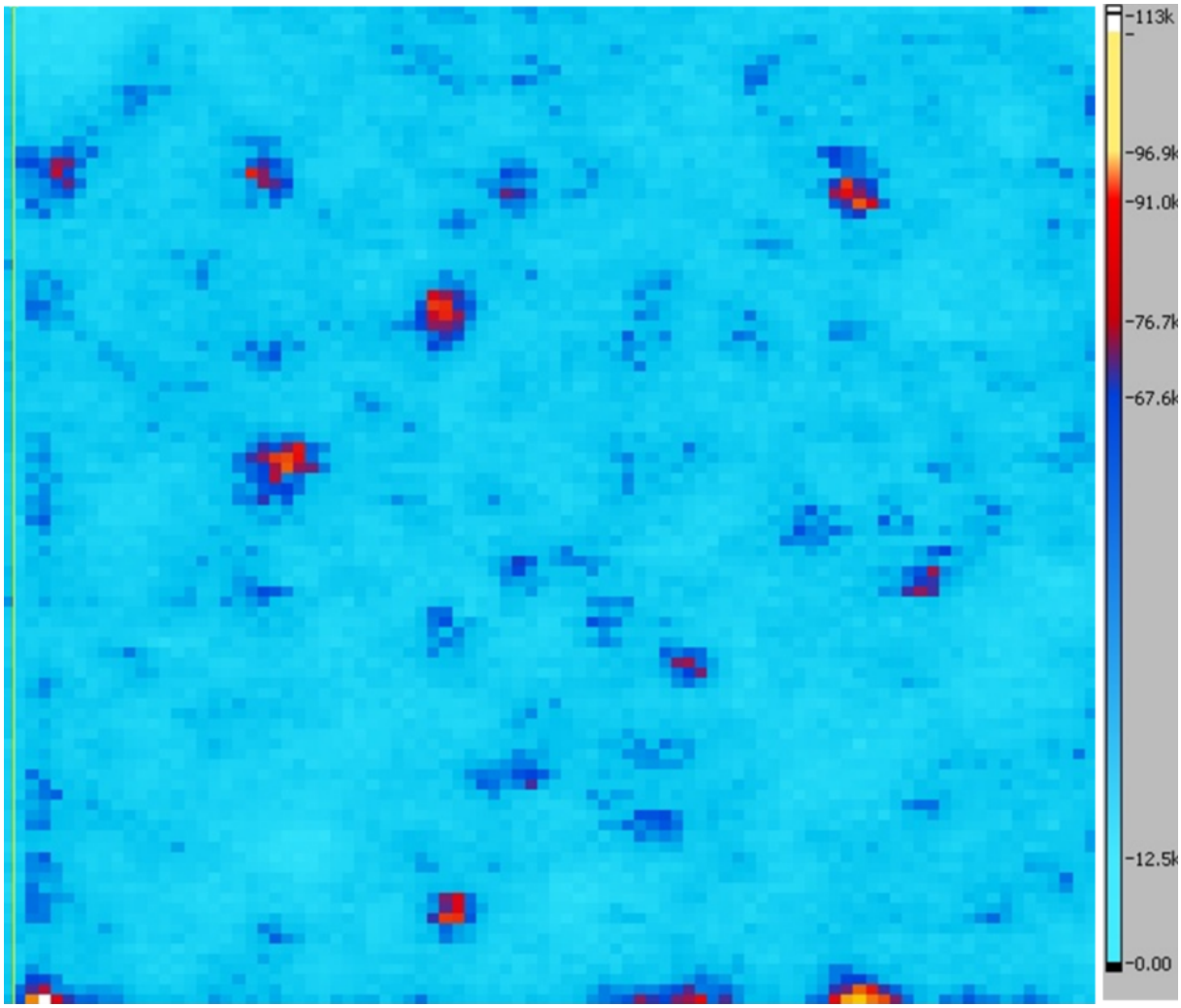

Figure S7. Single molecule detection on a recycled DLC-AAO membrane using confocal scanning microscopy (10×10 μm^2). The bright spots represent a single (or multiple) emission molecule(s) event(s) of the dyes attached to the captured DNA molecules. The DLC-AAO membrane was cleaned and washed with strong chemicals (boiling NaOH) , then its surface was functionalized with probe DNA and reused for DNA capture and sensing. It is confirmed that the functionality of the membrane has not being changed after recycling and re-functionalization.

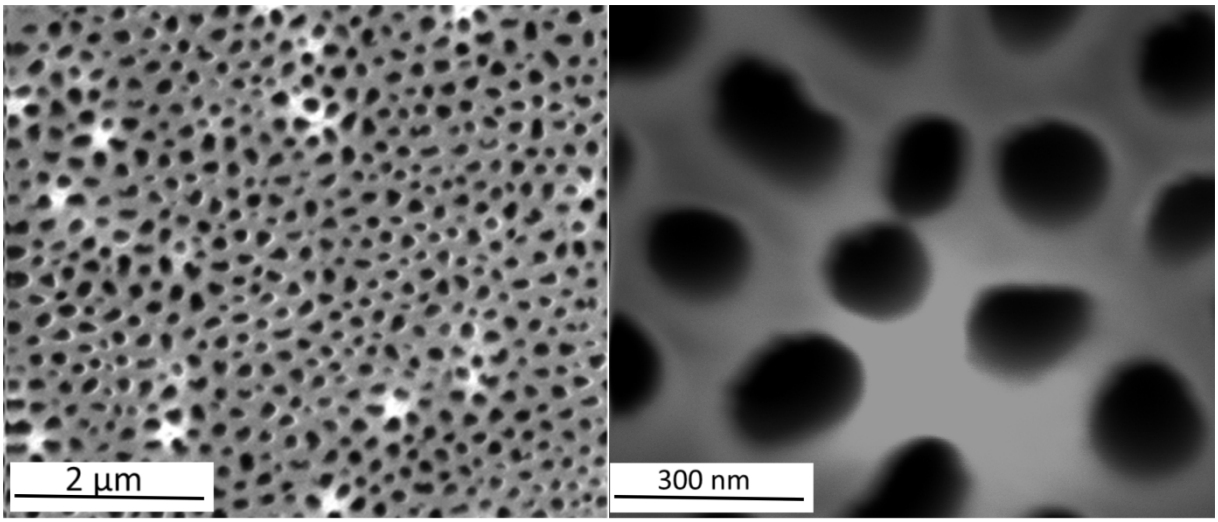

Figure S8. SEM images of the DLC-AAO membranes after oxygen plasma treatment. There is no apparent change in the structure of the DLC-AAO after the oxygen plasma or by other chemicals procedures.